Cardiomyocytes from AKAP7 knockout mice respond normally to adrenergic stimulation

Brian W. Jones[a], Sylvain Brunet[a,1], Merle L. Gilbert[a], C. Blake Nichols[a,2], Thomas Su[a], Ruth E. Westenbroek[a], John D. Scott[a,b], William A. Catterall[a,3], and G. Stanley McKnight[a,3]

[a]Department of Pharmacology and [b]Howard Hughes Medical Institute, University of Washington, Seattle, WA 98195

Contributed by William A. Catterall, September 5, 2012 (sent for review June 13, 2012)

Protein kinase A (PKA) is activated during sympathetic stimulation of the heart and phosphorylates key proteins involved in cardiac Ca^{2+} handling, including the L-type Ca^{2+} channel ($Ca_V1.2$) and phospholamban (PLN). This results in acceleration and amplification of the beat-to-beat changes in cytosolic Ca^{2+} in cardiomyocytes and, in turn, an increased rate and force of contraction. PKA is held in proximity to its substrates by protein scaffolds called A kinase anchoring proteins (AKAPs). It has been suggested that the short and long isoforms of AKAP7 (also called AKAP15/18) localize PKA in complexes with $Ca_V1.2$ and PLN, respectively. We generated an AKAP7 KO mouse in which all isoforms were deleted and tested whether Ca^{2+} current, intracellular Ca^{2+} concentration, or Ca^{2+} reuptake were impaired in isolated adult ventricular cardiomyocytes following stimulation with the β-adrenergic agonist isoproterenol. KO cardiomyocytes responded normally to adrenergic stimulation, as measured by whole-cell patch clamp or a fluorescent intracellular Ca^{2+} indicator. Phosphorylation of $Ca_V1.2$ and PLN were also unaffected by genetic deletion of AKAP7. Immunoblot and RT-PCR revealed that only the long isoforms of AKAP7 were detectable in ventricular cardiomyocytes. The results indicate that AKAP7 is not required for regulation of Ca^{2+} handling in mouse cardiomyocytes.

The key determinants of cardiac output—the force of contraction and rate of relaxation—are rooted in the amplitude and kinetics of Ca^{2+} transients that occur in individual cardiomyocytes. Adrenergic stimulation initiates cAMP-dependent signaling pathways that activate PKA leading to phosphorylation of numerous proteins that are critical for Ca^{2+} entry, release, and reuptake, as well as sarcomeric proteins more closely associated with contraction, such as myosin-binding protein C and troponin I. This phosphorylation amplifies Ca^{2+} influx through voltage-gated Ca^{2+} channels ($Ca_V1.2$ in the ventricle) and the corresponding increase in Ca^{2+}-induced Ca^{2+} release from the sarcoplasmic reticulum (SR) through ryanodine receptors augments contractility. Equally important is the enhanced removal of Ca^{2+} from the cytosol that allows the heart to relax more quickly during diastole, which is accomplished primarily by phosphorylating phospholamban (PLN), which in turn relieves PLN inhibition of the sarcoplasmic reticulum Ca^{2+} ATPase (SERCA).

Distinct, localized actions of PKA are coordinated in two ways: (*i*) cAMP production and hydrolysis are restricted by the subcellular localization of cyclases and phosphodiesterases, respectively, and (*ii*) PKA is directed to specific subcellular sites by binding to an assortment of protein scaffolds known as A kinase anchoring proteins (AKAPs) (1). By directing PKA to specific subcellular sites, AKAPs determine not only the specificity of protein phosphorylation, but also the speed with which these systems respond to adrenergic stimulation. Some AKAPs are implicated in clinically relevant cardiac signaling events (2–4). For example, regulation of potassium channel current in the heart depends on formation of complexes containing AKAP9 (yotiao), PKA, and the I_{Ks} potassium channel α subunit (KCNQ1); an inherited single point mutation in AKAP9 impairs AKAP9–KCNQ1 interaction and ultimately leads to long QT syndrome (4).

AKAP7 is expressed as a family of alternatively spliced anchoring proteins that bind all isoforms of PKA regulatory subunit, albeit with different affinities. The shortest variant, AKAP7α, was detected as a protein band that copurified with rabbit skeletal muscle L-type Ca^{2+} channel, $Ca_V1.1$, and interacted with purified PKA–RII in a far Western assay (5). Because the band ran at 15 kDa, it was named AKAP15. Another study identified a cDNA from a human fetal brain expression library that encoded a novel RII-binding protein of 81 aa, reported as AKAP18 (6). Further cloning and mass spectrometry revealed that AKAP15 and AKAP18 are the same protein arising from the *Akap7* gene (6, 7). To date, four different transcripts of *Akap7* have been identified in several species that are translated into specific polypeptides designated by increasing length as α, β, γ, and δ (Fig. 1) (5, 6, 8, 9).

The functional significance of AKAP7α was determined by several studies that looked at its role in regulating ion channel activity. Direct interaction between AKAP7α and L-type Ca^{2+} channels was shown to rely on a modified leucine zipper (LZ) domain found in all AKAP7 isoforms, and competing peptides based on this interacting sequence prevented PKA regulation of endogenous Ca^{2+} channels in cardiac and skeletal muscle cells (10, 11). In addition to copurifying with rabbit skeletal muscle L-type Ca^{2+} channel (5), AKAP7α was shown to modulate cardiac or skeletal L-type Ca^{2+} channels exogenously expressed in cultured cells (6, 12) and to copurify with and modulate rat brain voltage-gated Na^{2+} channels (13–15). Based on its requirement for reconstitution of cAMP-regulation of Cav1.2 channels in nonmuscle cells, it was proposed that AKAP7α is required for normal adrenergic up-regulation of L-type Ca^{2+} current in cardiomyocytes (11, 12).

The longest isoform, AKAP7δ, was also reported to affect intracellular Ca^{2+} in cardiomyocytes, but in this case via indirect regulation of SERCA via PLN (16). AKAP7δ in rat heart binds to PLN and coordinates its phosphorylation by PKA. A recent study reported that AKAP7δ in rat heart also coordinates PKA phosphorylation of inhibitor-1 (17), which in turn inhibits protein phosphatase 1 (18). Because protein phosphatase 1 is the major phosphatase responsible for dephosphorylating PLN (18, 19), this suggests that the long isoforms of AKAP7 may coordinate both phosphorylation and dephosphorylation of PLN.

These reports suggest that genetic deletion of AKAP7 would result in decreased phosphorylation of cardiac $Ca_V1.2$ and PLN in response to adrenergic stimulation and manifest phenotypes related to impaired cardiac Ca^{2+} handling in two ways: first, by decreased Ca^{2+} entry through $Ca_V1.2$; and second, by slowed Ca^{2+} reuptake via SERCA. We generated a whole animal knockout of AKAP7 by targeting the RII-binding and ion channel interaction exon shared by all four isoforms and examined Ca^{2+} channel regulation and protein phosphorylation in isolated adult ventric-

Author contributions: B.W.J., S.B., J.D.S., W.A.C., and G.S.M. designed research; B.W.J., S.B., M.L.G., C.B.N., and T.S. performed research; T.S. and R.E.W. contributed new reagents/analytic tools; B.W.J. and S.B. analyzed data; and B.W.J. and G.S.M. wrote the paper.

The authors declare no conflict of interest.

[1]Present address: Department of Neurosciences, The Cleveland Clinic Foundation, Cleveland, OH 44195.

[2]Present address: Department of Pharmacology, University of California, Davis, CA 95616.

[3]To whom correspondence may be addressed. E-mail: wcatt@u.washington.edu or mcknight@u.washington.edu.

This article contains supporting information online at www.pnas.org/lookup/suppl/doi:10.1073/pnas.1215219109/-/DCSupplemental.

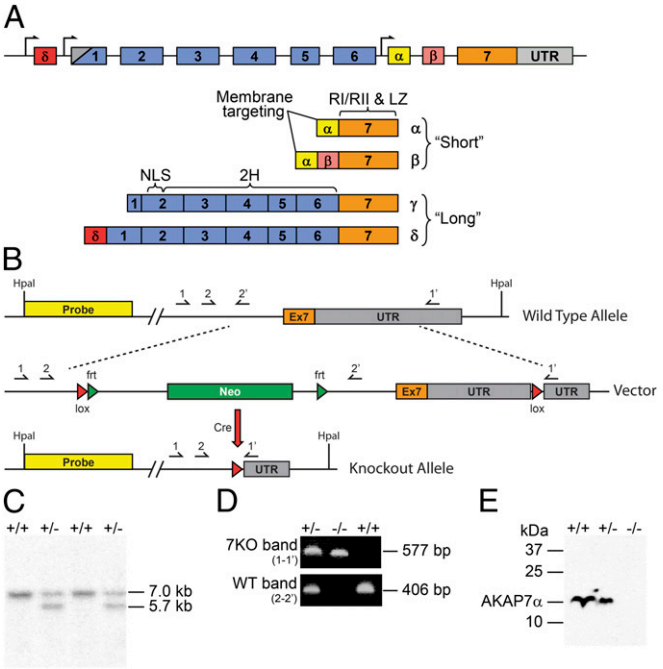

Fig. 1. Genetic disruption of all four *Akap7* splice variants. (*A*) Nonscaled model of *Akap7* gene showing 10 known exons and three presumed promoters that lead to four unique splice variants, broadly grouped as short (α and β) or long (γ and δ) isoforms. Exon 7 is the only exon shared by all splice variants and contains the PKA binding (RI/RII) domain and modified leucine zipper motif (LZ). Palmitoylation and myristoylation of N-terminal residues in exon α confer membrane targeting; long isoforms contain a nuclear localization sequence (NLS) and 2H phosphoesterase domain. (*B*) Diagram of *Akap7* knockout strategy, which targets exon 7, including the 3′-UTR. Restriction sites, Flp and Cre recombination sites, and location of PCR primers are shown. (*C*) Southern blot of HpaI-cut DNA from *Meox2*$^{+/Cre}$ x *Akap7*$^{+/lox}$ mice, (*D*) PCR using specific primers, and (*E*) immunoblot of brain lysate to confirm successful disruption of *Akap7* probed with GST-AKAP15 antibody (7).

ular myocytes stimulated with the β-adrenergic agonist isoproterenol (ISO). Surprisingly, we found that deletion of AKAP7 does not result in deficits in adrenergic stimulation of Ca^{2+} handling or phosphorylation of PLN or $Ca_V1.2$. Moreover, using both Western blot and RT-PCR we found that although AKAP7γ/δ are expressed in cardiomyocytes, there is no detectable expression of AKAP7α/β in isolated cardiomyocytes from mouse or rat.

Results

Generation of AKAP7 KO Mice. Four splice variants of *Akap7* exist that apparently arise from three separate promoters (Fig. 1*A*). To disrupt expression of all isoforms, we used Cre/loxP recombination to delete the only common exon, which we refer to as exon 7 (Fig. 1*B*). This exon contains the modified leucine zipper domain that directs binding to Ca^{2+} and Na^{2+} channels, the RI/RII-binding domain that defines it as an AKAP, and the 3′-UTR. If any transcribed mRNA is still translated it would produce a truncated protein lacking the critical AKAP domain. Successful recombination and deletion was confirmed by Southern blot and PCR (Fig. 1 *C* and *D*). AKAP7 KO animals are fertile and healthy and exhibit no obvious phenotype. Disruption of protein expression was confirmed by immunoblotting brain lysates with an antibody characterized previously against AKAP7 (Fig. 1*E*) (7).

Expression of AKAP7 Protein and mRNA in Various Tissues. Several studies have reported AKAP7 expression in various tissues by Northern blot of rat or human tissue (6–9). At least two AKAP7 transcripts exist (of 2.4 and 4.3 kb), and there are notable differences in their tissue-specific expression among species (6–9). Thus, we performed immunoblots and RT-PCR with mouse tissues to clarify where AKAP7 is expressed in mouse and to better predict the effect of its deletion in the KO animal. We also isolated adult ventricular cardiomyocytes—the focal cell type of our study—so we could avoid contamination from other cell types in the whole heart; i.e., fibroblasts, nervous tissue, vasculature, etc.

An antibody raised against a GST fusion of AKAP7α has been used previously to probe for AKAP7α in heart lysates by immunoblot (7, 11). This antibody detected AKAP7α in brain lysates, but also detected a nonspecific band near 15 kDa in KO heart lysates, which interfered with interpretation of protein expression (Fig. S1). Due to this concern over antibody specificity, we switched to a different anti-AKAP7 antibody (Proteintech; 12591-1) that does not detect low molecular weight nonspecific bands in heart. Two faint bands at ~37 and ~42 kDa were detected by imunoblot in all WT but not KO tissue lysates and correspond to the reported molecular weights of AKAP7γ and AKAP7δ, respectively (Fig. 2*A*). A 15-kDa protein, AKAP7α, was highly expressed only in brain and weakly in lung lysates from WT animals. It was possible that our inability to detect AKAP7α in some tissues was due to very low expression levels, so we immunoprecipitated protein from tissue extracts to concentrate and enrich AKAP7. We were able to enhance the AKAP7α signal from brain and lung and detect very faint bands in heart tissues, but isolated cardiomyocytes, skeletal muscle, and kidney inner medulla still showed no AKAP7α (Fig. 2*B*).

We used quantitative RT-PCR as a more sensitive method to detect expression of AKAP7 (Fig. 2 *C* and *D*). Our PCR probes distinguish short from long isoforms, but do not distinguish AKAP7α from AKAP7β or AKAP7γ from AKAP7δ. AKAP7 mRNA levels agreed qualitatively with the immunblots: AKAP7γ/δ were detected in all tissues whereas AKAP7α/β were only appreciably detected in brain, with some very low expression in crude heart extracts. Importantly, there was no detectable AKAP7α/β mRNA in isolated cardiomyocytes even after 40 reaction cycles. We likewise observed no AKAP7α protein or mRNA in isolated adult rat ventricular cardiomyocytes using similar methods (Fig. S2).

β-Adrenergic Stimulation of $Ca_V1.2$ Phosphorylation Is Normal in AKAP7 KO Cardiomyocytes. The fact that AKAP7α is not detectable in murine cardiomyocytes led us to hypothesize that it is not required for regulating $Ca_V1.2$ in this cell type. However, the long isoforms are expressed in cardiomyocytes and contain the same leucine zipper domain (Fig. 1*A*) shown to be essential for AKAP7α–$Ca_V1.2$ interaction in vitro, so we examined whether AKAP7 deletion impaired normal $Ca_V1.2$ function.

Isolated adult ventricular cardiomyocytes were stimulated in vitro with increasing concentrations of ISO (0.1–1,000 nM) and collected for SDS/PAGE and immunoblot. There were no differences between WT and KO in the amount of $Ca_V1.2$ expressed when normalized to GAPDH and the degree of phosphorylation of $Ca_V1.2$–Ser1928 was identical for WT and KO at all concentrations of agonist (Fig. 3). Although this site is not essential for regulating $Ca_V1.2$ function (20), it is an established PKA phosphorylation site and reflects activation of PKA in close proximity to $Ca_V1.2$ (21).

β-Adrenergic Stimulation of Ca^{2+} Current Is Not Diminished in AKAP7 KO Cardiomyocytes. ISO-induced amplification of L-type Ca^{2+} current (I_{Ca}) was normal in AKAP7 KO myocytes and ISO stimulation was associated with a leftward shift in L-type Ca^{2+} current–voltage relationship similar to that seen in WT cardiomyocytes (Fig. 4). AKAP5 (also called AKAP79/150) is also expressed in heart and has been shown to interact with $Ca_V1.2$ (22–25). To rule out compensation by AKAP5 in AKAP7 KOs, we measured ISO stimulation of Ca^{2+} current in AKAP5/7 double knockout (DKO) cardiomyocytes and found no differences in whole-cell current compared with WT (Fig. 4). Cardiomyocytes

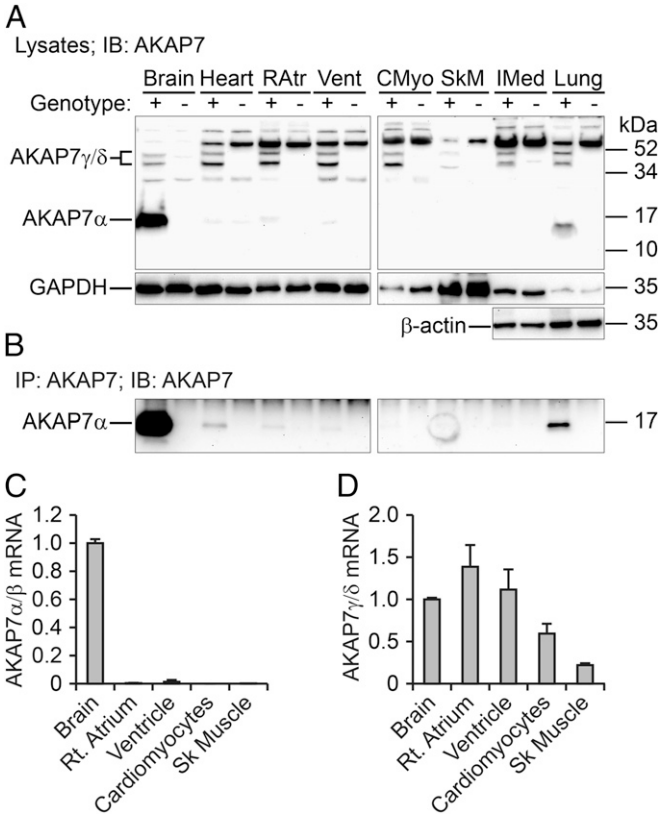

Fig. 2. AKAP7α is expressed in brain but not in cardiomyocytes or skeletal muscle. (*A*) Lysates of various tissues from WT or AKAP7 KO mice were probed by immunoblot using rabbit polyclonal anti-AKAP7 antibody 12591-1. Long isoforms, ~37–42 kDa, are faintly detected in all WT tissues. Some nonspecific bands (e.g., ~55 kDa) are observed in tissue from WT and KO animals. Total protein was measured by BCA assay and 80 μg were loaded per lane; GAPDH and β-actin are shown as additional loading controls. (*B*) AKAP7 was immunoprecipitated from lysates using guinea pig anti-AKAP7 YO869 antibody to enrich protein before probing via immunoblot as above. The single band at 15 kDa corresponds to AKAP7α and is only weakly detected in nonbrain tissues. *RAtr*, right atrium; *Vent*, ventricle; *CMyo*, isolated cardiomyocytes; *SkM*, skeletal muscle (quadriceps); *IMed*, kidney inner medulla. (*C* and *D*) Quantitative RT-PCR using Taq-Man MGB probes detected AKAP7 long isoforms in all tissues, but short isoforms only appreciably in the brain.

of all three genotypes had a similar capacitance and vehicle-treated current–voltage relationship (Fig. S3). Together, these findings show that there is no requirement for any isoforms of AKAP7 in $Ca_V1.2$ regulation and suggest that another AKAP fulfills this role in mouse cardiomyocytes. Additionally, PKA RIIα coimmunoprecipated with $Ca_V1.2$ from WT, 5KO, 7KO, and DKO heart, indicating that the two proteins are part of a complex that does not require AKAP5 or AKAP7 (Fig. S4). RII overlay on AKAP5/7 DKO heart lysates did not reveal upregulation of any AKAPs that might compensate for loss of AKAP5 and/or AKAP7 (Fig. S5).

β-Adrenergic Regulation of PLN Phosphorylation/Dephosphorylation and Ca^{2+} Transients Is Unaffected in AKAP7 KO Cardiomyocytes. Published reports propose a model where AKAP7γ/δ coordinates a multimolecular complex including PKA, inhibitor-1, and protein phosphatase 1 in the regulation of PLN (16, 17). We tested this model by stimulating isolated adult ventricular cardiomyocytes in vitro with increasing concentrations of ISO (0.1–1,000 nM) and analyzing phosphorylated PLN by immunoblot. There were no differences between WT and KO in the amount of PLN expressed when normalized to GAPDH. Phosphorylation of PLN in AKAP7 KO cardiomyocytes was normal for all concentrations of agonist as detected with a phospho–site-specific antibody against the PKA target site on PLN, Ser16 (Fig. 5 *A* and *B*). To test the role of AKAP7γ in coordinating the dephosphorylation of PLN, we stimulated cardiomyocytes in vitro with ISO for 7 min before adding the β-adrenergic antagonist propranolol (1 μM) and monitoring the decay of phospho-Ser16 on PLN. Phosphorylation of PLN decayed with a half-life of 2 min and there was no difference between WT and KO cardiomyocytes in the rate or extent of dephosphorylation of PLN over 16 min (Fig. 5 *C* and *D*).

PLN is primarily a negative regulator of SERCA, and relief of this inhibition following adrenergic stimulation is the primary cause of increased peak intracellular Ca^{2+} during contraction and rapid Ca^{2+} reuptake into the SR during relaxation (26). We asked whether AKAP7 KO cardiomyocytes displayed altered Ca^{2+} handling by measuring intracellular Ca^{2+} concentrations with the Ca^{2+} indicator Fluo-4 in isolated cardiomyocytes paced at 1 Hz. We observed no difference in the basal or ISO-stimulated amplitude of the Ca^{2+} transient or in the rate of reuptake of Ca^{2+} into the SR (Fig. 5 *E* and *F*). In summary, we found no evidence that AKAP7 is required for PLN–SERCA regulation.

Phosphorylation of $Ca_V1.2$ and PLN Requires PKA. Having observed that AKAP7 is not required for normal $Ca_V1.2$ or PLN activity or phosphorylation, we considered whether another kinase might compensate in AKAP7 KO. We repeated experiments that measured phosphorylation of $Ca_V1.2$ and PLN, this time incubating the isolated cardiomyocytes with PKA inhibitors before the application of ISO. H89 blocks PKA by competitive inhibition of the ATP-binding site on the catalytic subunit and 8-(4-chlorophenylthio)adenosine-3′,5′-cyclic monophosphorothioate, Rp-isomer) (Rp-8-CPT-cAMPS) occupies the cAMP-binding site on the PKA regulatory subunit but does not promote holoenzyme dissociation. Both PKA inhibitors significantly inhibited phosphorylation of PLN and $Ca_V1.2$ and the degree of inhibition was identical between genotypes (Fig. 6), indicating that PKA activity is responsible for these phosphorylation events and that KO cardiomyocytes do not use an alternative or compensatory pathway.

Discussion

Peptides derived from the PKA-binding domain of an AKAP can be used to competitively inhibit PKA anchoring, and several reports have used this technique to establish the involvement of AKAPs in cardiac Ca^{2+} handling. Adenovirally expressed Ht31 (derived from AKAP13) (27) in rat hearts reduced PLN phosphorylation (28) as did treatment of isolated rat cardiomyocytes in vitro with AKAD (derived from AKAP10) (29). Conversely, the small molecule, 3,3′-diamino-4,4′-dihydroxydiphenylmethane

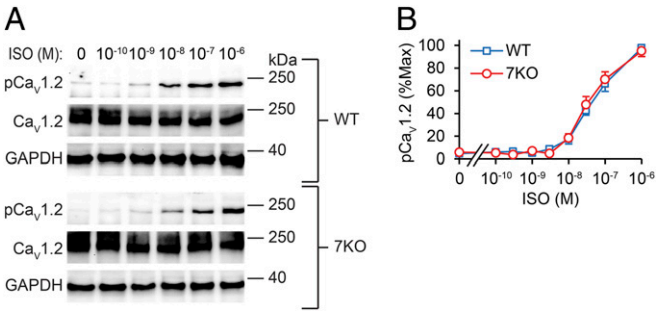

Fig. 3. Adrenergic stimulation results in phosphorylation of $Ca_V1.2$ in AKAP7 KO cardiomyocytes. (*A*) Isolated cardiomyocytes from WT or AKAP7 KO were stimulated with increasing concentrations of ISO for 7 min and phosphorylated $Ca_V1.2$ (Ser1928) was detected by immunoblot. (*B*) Densitometry of immunoblots from at least three experiments showed no difference between WT and KO. Values were normalized to percent maximum to allow comparison between experiments; shown are SEM.

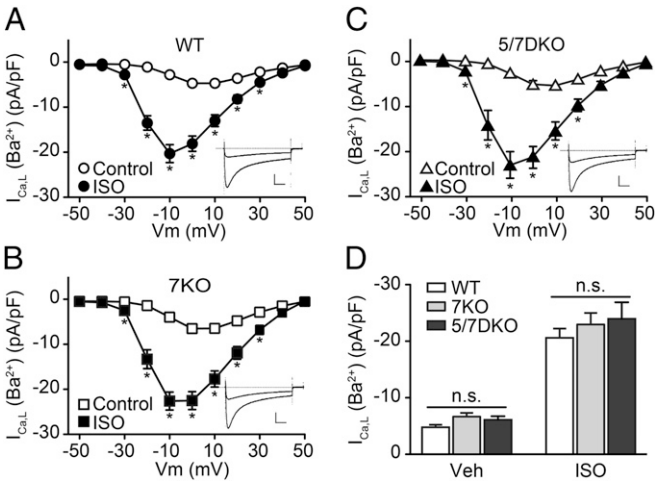

Fig. 4. L-type Ca^{2+} channel current is up-regulated by adrenergic stimulation in AKAP7 KO cardiomyocytes. (*A–C*) Effect of ISO (1 μM) on L-type Ca^{2+} current–voltage relationship recorded from (*A*) WT, (*B*) AKAP7 KO, or (*C*) AKAP5/7 double knockout (DKO) cardiomyocytes. *Inset*, single-cell traces. (Scale bar, 5 pA/pF and 50 ms.) Shown are SEM; *$P < 0.01$ by Student *t* test. (*D*) Comparison of calcium current recorded from vehicle- or ISO-treated cardiomyocytes. Shown are SEM; NS, $P > 0.05$.

(FMP-API-1), which simultaneously activates anchored PKA as it disrupts anchoring, caused increased PLN phosphorylation (30). Disrupting peptides introduced via patch pipette blunt the effect of ISO on whole-cell Ca^{2+} current (I_{Ca}) in neonatal rat or adult rat or mouse cardiomyocytes (11, 31, 32). Another peptide, derived from the leucine zipper domain on AKAP7 and designed to competitively inhibit AKAP–$Ca_V1.2$ interaction, has a similar effect (11). These approaches demonstrate that PKA anchoring near $Ca_V1.2$ and PLN is essential in mouse and rat cardiomyocytes and that the required AKAP interacts via the modified leucine zipper motif. However, these results do not reveal the identity of the specific AKAP if more than one AKAP can interact via the modified leucine zipper motif. The prevailing models identify AKAP7 or possibly AKAP5 as the critical AKAP (1, 33–37).

Previous evidence supported the conclusion that AKAP7α anchors PKA to $Ca_V1.1$ or $Ca_V1.2$ in skeletal and heart muscle. Mass spectrometry of the 15-kDa band copurifying with $Ca_V1.1$ from rabbit skeletal muscle identified it as AKAP7α (7). Cotransfection of $Ca_V1.2$ and AKAP7α in heterologous cells results in ISO-sensitive Ca^{2+} currents, whereas transfection with $Ca_V1.2$ alone does not (12). Cotransfection of $Ca_V1.2$ with a mutated AKAP7α lacking lipid-modified residues essential for membrane targeting does not preserve ISO-sensitive I_{Ca} (6) and the AKAP7-leucine zipper peptide disrupts ISO up-regulation of Ca^{2+} current (11). Furthermore, an antibody raised against a GST fusion of AKAP7α detects a 15-kDa band that coimmunoprecipitates with endogenous Ca^{2+} channel from rabbit skeletal muscle and also detects a 15-kDa band in rat and mouse heart (7, 10, 11). These results all supported the conclusion that AKAP7 was required for Ca^{2+} channel regulation in cardiac and skeletal muscle.

In contrast to the conclusions of these extensive previous studies, our results with KO tissues as a negative control revealed that AKAP7α is not required for Ca^{2+} channel regulation in mouse heart because AKAP7 KO cardiomyocytes had normal whole-cell Ca^{2+} current (Fig. 4) and AKAP7α was not detected in dissociated cardiac myocytes by the sensitive methods used here (Fig. 2 and Fig. S2). The fact that AKAP7 was previously identified in rabbit skeletal muscle by mass spectrometry (7) but is not detectable in murine skeletal muscle (Fig. 2 and Fig. S2) raises the question of whether there are differences in AKAP7α expression between species. Alternatively, the presence of small amounts of AKAP7α in mouse heart lysates, but not in isolated cardiomyocytes, suggests that the protein is expressed in nonmuscle cells in complex tissues. Therefore, it will be important in future studies to measure AKAP7α protein and mRNA in isolated cardiac and skeletal myocytes from multiple species, including human.

Biochemical and physiological approaches in this report also show that AKAP7γ/δ is not essential for normal Ca^{2+} handling because AKAP7 KO cardiomyocytes were normal in all parameters tested. Clearly this does not preclude any AKAP7γ/δ interaction with PLN, but does suggest that another unidentified AKAP is primarily responsible for anchoring PKA in PLN–SERCA complexes. Thus, our data call for reexamination of the established model and suggest that other AKAPs are responsible for anchoring PKA near $Ca_V1.2$ and PLN.

At least 14 AKAPs have been detected in heart, although it is not clear how many are in cardiomyocytes specifically (1, 33–37). A modified leucine zipper domain in AKAP5 and AKAP7 is essential for direct interaction with $Ca_V1.2$ expressed in heterologous cells (11, 25). In this study we show that neither AKAP5 nor AKAP7 are required for PKA anchoring to $Ca_V1.2$ in cardiomyocytes. Nevertheless, the fact that a leucine zipper peptide disrupts up-regulation of Ca^{2+} current in cardiomyocytes (11) suggests that the relevant AKAP in cardiomyocytes likewise contains a leucine zipper. Candidate AKAPs include AKAP6 (mAKAP) (38), AKAP9 (yotiao) (39), and possibly AKAP13 (AKAP-Lbc) (40).

Because the short form of AKAP7, AKAP7α, was not detectable in mouse or rat cardiomyocytes, its contribution to PKA anchoring in other tissues will be the focus of future studies. AKAP7α is highly expressed in the brain (Fig. 2) and was shown to copurify with brain sodium channels (13, 14, 41) and Ca^{2+}

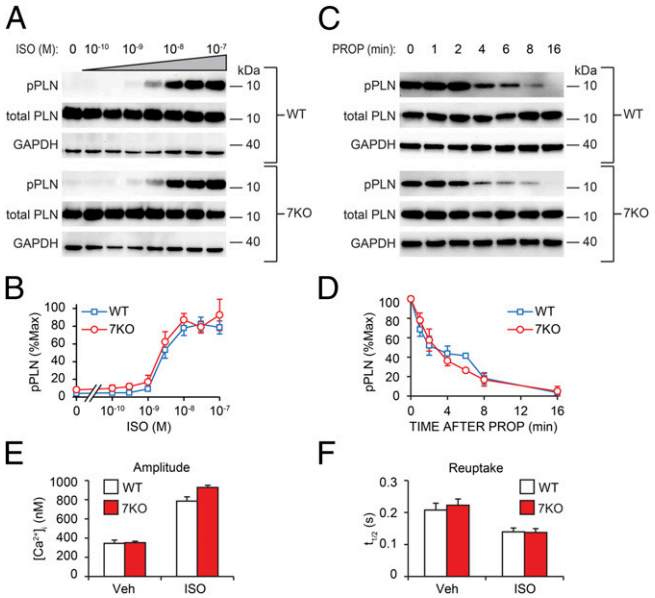

Fig. 5. Adrenergic stimulation evokes PLN phosphorylation and improved Ca^{2+} handling in AKAP7 KO cardiomyocytes. (*A* and *B*) Isolated cardiomyocytes from WT or AKAP7 KO were stimulated with increasing concentrations of ISO for 7 min and phosphorylated PLN (Ser16) was detected by immunoblot; SEM from at least three independent experiments are shown. (*C* and *D*) Isolated cardiomyocytes were stimulated with ISO (30 nM) for 10 min and dephosphorylation was initiated upon addition of propranolol (1 μM) to block β-adrenergic receptor signaling for the indicated times. (*E*) Effect of ISO (100 nM) on Ca^{2+} transient peak amplitude or (*F*) half-time of Ca^{2+} reuptake in paced isolated cardiomyocytes; shown are SEM of three independent experiments wherein at least five cells were recorded. Differences between genotypes were not significant ($P > 0.05$), whereas the effect of ISO was significant ($P < 0.01$) by two-way ANOVA.

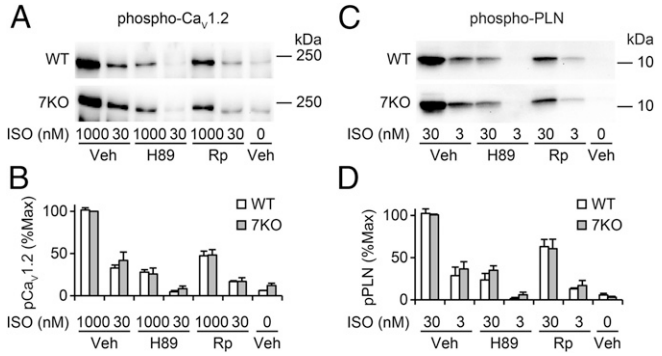

Fig. 6. Phosphorylation of $Ca_V1.2$ and PLN depends on PKA in AKAP7 KO. Isolated cardiomyocytes were incubated with H89 (100 μM) for 30 min or 8-CPT-Rp-CAMPS (1 mM) for 45 min before stimulation with 3–1,000 nM ISO for 7 min. (*A* and *B*) Phosphorylated $Ca_V1.2$ and (*C* and *D*) phosphorylated PLN were detected by immunoblot and quantified by densitometry; shown are SEM from three independent experiments. Differences between genotypes were not significant ($P > 0.05$) under any condition, whereas the effect of H89 or 8-CPT-Rp-CAMPS was significant ($P < 0.01$) for all concentrations of ISO by two-way ANOVA.

channels (42). AKAP7α has not been reported to interact with any proteins other than ion channels and PKA. It will be of interest to use our AKAP7 KO mouse to analyze the functional role of this AKAP in ion channel regulation in the brain.

Materials and Methods

Generation of KO Mice. The KO vector shown in Fig. 1*B* contained an frt-flanked neomycin resistance gene placed in the intron before exon 7 with loxP sites inserted upstream of the neo cassette and downstream of the coding region of exon 7. A chimeric (65%) male was crossed with C57/Bl6 females and their $Akap7^{+/lox}$ offspring were crossed with $Meox2^{+/Cre}$ males to delete the floxed exon 7 in the germ line. DNA isolated from $Meox2^{+/Cre} \times Akap7^{+/lox}$ mice was cut with HpaI and probed by Southern blot as described (43), revealing a 5.7-kb band diagnostic of the recombined gene. Heterozygotes were also identified by PCR (Fig. 1 *C* and *D*), back-crossed onto C57/Bl6 for seven generations, and crossed to yield WT and AKAP7 KO littermates. AKAP5 KO mice (44) were crossed to AKAP7 KO mice to generate AKAP5/7 DKO mice, which were healthy and fertile. All protocols were approved by the University of Washington Institutional Animal Care and Use Committee.

Southern Blotting and PCR. Southern blot analysis identified positive ES clones using a 672-bp probe located 3426 bases upstream of the exon 7 splice site. Southern blots detected HpaI fragments of 7 kb in wild type and 5.7 kb in KO.

For routine genotyping, tail DNA was purified using the NucleoSpin Tissue kit (Macherey-Nagel) and analyzed by PCR with DreamTaq DNA Polymerase (Fermentas) using the following primers: KO allele, 5′-TATTCCCAGCCGTGCTAACAC-3′ (forward) and 5′-TCTTGGCCTGAGTCTCAGGCT-3′ (reverse); WT or floxed allele, 5′-TGACCCTTTGCTGTGACTTC-3′ (forward) and 5′-TAGCTCTGCGCTCCTCTCTC-3′ (reverse).

Total RNA was isolated from freshly dissected mouse tissues using the RNeasy kit (Qiagen) and quantitative RT-PCR was performed using the SuperScript One-Step system (Invitrogen) and TaqMan MGB probes (Applied Biosystems). Oligonucleotides for mouse were: AKAP7 short isoforms, 5′-GCTTCCCTTTCGCCAGAGA-3′ (forward), 5′-CCTTGAGCACGGCGTTCT-3′ (reverse), and 6-FAM-AGGCTCAGTAAGAGGC(MGB); and long isoforms, 5′-ACTATTTCCTGTCCATTCCGATCAC-3′ (forward), 5′-TGCTGTAGTATCGAATTTTGCAAGAC-3′ (reverse), and 6-FAM-AGATTACAACCGGAATTAA(MGB).

Rat tissues were dissected, frozen in liquid nitrogen, and stored at −80 °C for later processing. Total RNA was isolated using the RNeasy kit and RT-PCR was performed using the Brilliant II SYBR mix (Agilent). AKAP7 short isoform primers were: 5′-GCTTCCCCTTCGCCAGAGA-3′ (forward) and 5′-CCTTGAGCACGGCGTTCT-3′ (reverse).

PCR reactions were carried out for 40 cycles following an initial 30-min reverse transcription on an Mx300P Thermocycler (Stratagene). Reaction products were run on gels to confirm the presence of only one appropriately sized band. Reaction efficiencies, determined using a standard dilution of brain RNA, were 100% for short isoforms and 88% for long isoforms. Values were normalized to the amount detected in brain and replicates from at least three independent experiments were averaged ±SEM.

RII Overlay, Immunblotting, and Immunoprecipitation. [^{32}P]-RIIα overlay was performed essentially as described (45). Tissues for immunoblot were homogenized using a Polytron in buffer (20 mM Tris, 150 mM NaCl, 5 mM EGTA, 5 mM EDTA, 5 mM NaF, pH 7.6, 1% Triton X-100, 0.5% deoxycholic acid, 0.1% SDS) and protease inhibitor mixture (Sigma). Lysates were centrifuged at 3,000 × *g* for 10 min at 4 °C and supernatant was collected and diluted to 2 mg/mL based on the bicinchoninic acid (BCA) protein assay (Pierce) in sample buffer [NuPAGE lithium dodecylsulfate (LDS) sample buffer (Invitrogen), 100 mM DTT, 3% (vol/vol) β-mercaptoethanol]. For immunoprecipitation, 2 mg of lysate was diluted in 1 mL of buffer and rotated at 4 °C overnight with 4 μg rabbit anti-$Ca_V1.2$ antibody CNC1 (46), 4 μg rabbit anti-RIIα (sc-909; Santa Cruz), or 6 μg of guinea pig anti-AKAP7 antibody YO869. This guinea pig antibody was generated by New England Peptide using a peptide derived from the first 19 aa of the mouse sequence of exon 7, EKDRREPEDAELVRLSKRL. YO869 was affinity purified against the immunizing peptide using the SulfoLink kit (Pierce). Fifty microliters each of PureProteome magnetic protein A and G beads (Millipore) were added for 1 h to bind antibody complexes and samples were washed twice with buffer before being resuspended in 75 μL of sample buffer.

Protein samples were heated at 85 °C for 15 min, loaded on 8% (for $Ca_V1.2$) or 15% (for AKAP7 or PLN) SDS/PAGE gels, and transferred to Whatman nitrocellulose (for $Ca_V1.2$) or Millipore 0.2 μm PVDF (for AKAP7 or PLN). Membranes were blocked in 5% (wt/vol) BSA in TBS-T [25 mM Tris-Cl (pH 7.6), 150 mM NaCl, 0.1% Tween 20] and incubated at 4 °C overnight with the following primary antibodies: 1:25,000 mouse anti–β-actin clone AC-74 (Sigma), 4 μg/mL rabbit anti-AKAP7 (GST-AKAP15) (7), 0.16 μg/mL rabbit anti-AKAP7 (12591-1; Proteintech), 1.5 μg/mL rabbit anti-$Ca_V1.2$ phosphoserine 1928 (CH3P) (46), 0.9 μg/mL rabbit anti-$Ca_V1.2$ (CNC1) (46), 0.2 μg/mL mouse anti-GAPDH (AM4300; Ambion), 0.125 μg/mL mouse anti-PLN (Badrilla), 0.1 μg/mL rabbit anti-PLN phosphoserine 16 (Badrilla), or 0.04 μg/mL rabbit anti-RIIα (sc-909; Santa Cruz). Blots were washed five times in TBS-T and incubated for 1 h at room temperature with appropriate HRP-conjugated secondary antibodies (Jackson Labs) in 5% (wt/vol) BSA. HRP-conjugated secondary antibody was detected with SuperSignal West Pico or Dura chemiluminescent substrate (Pierce) and images were acquired and analyzed on a Kodak Image Station 440. Phospho-$Ca_V1.2$ or phospho-PLN were normalized to GAPDH in individual experiments and values for each condition expressed as the percent maximum within that experiment; these values were pooled and shown as mean ±SE. The amount of total $Ca_V1.2$ or PLN did not differ between genotypes, as assessed by normalizing to GAPDH.

Cardiomyocyte Isolation and Culture. Adult ventricular cardiomyocytes from mouse or rat were isolated by enzymatic digestion and gentle dissection essentially as described (47). Cells used for Ca^{2+} transients were maintained in external control solution (140 mM NaCl, 5 mM KCl, 1 mM $MgCl_2$, 2 mM $CaCl_2$, 10 mM glucose, 10 mM Hepes, pH 7.4) at room temperature for 0.5–3 h. Cells used for phosphorylation assays were plated at ∼50,000 cells per dish in laminin-coated dishes in M199 media with Hanks' salts (Invitrogen) supplemented with GlutaMAX (Invitrogen) and penicillin/streptomycin and incubated at 37 °C in 5% CO_2 and 95% humidity for 1 h before treatment.

In Vitro Phosphorylation and Dephosphorylation of PKA Substrates. Cultured isolated cardiomyocytes were stimulated by addition of a 20% volume of ISO in culture media for 7.5 min at 37 °C. To inhibit PKA phosphorylation, cells were incubated with 100 μM H89 (Calbiochem) for 30 min or 1 mM 8-CPT-Rp-cAMPS (Biolog) for 45 min before addition of ISO for 7.5 min. Dephosphorylation was initiated by adding 1 μM propranolol to cells that had been stimulated for 10 min with ISO. All reactions were stopped by lysing the cells in 300 μL ice-cold sample buffer.

Electrophysiology. Electrophysiological recordings were obtained as previously published (48). In brief, patch pipettes (2.5–3.5 MΩ) were pulled from micropipette glass (VWR Scientific) and fire polished. Currents were recorded with an Axopatch 200B amplifier (Molecular Devices) and sampled at 5 kHz after anti-alias filtering at 2 kHz. Data acquisition and command potentials were controlled by Pulse 8.50 (HEKA Elektronik) and data were stored for off-line analysis. Voltage protocols were delivered at 10-s intervals, and leak and capacitive transients were subtracted using a P/4 protocol. Approximately 80% of series resistance was compensated with the voltage-clamp amplifier circuitry.

For whole-cell voltage clamp recordings of $I_{Ca,L}$ with Ba^{2+} as charge carrier [$I_{Ca,L}(Ba^{2+})$] the extracellular solution contained: 1.8 mM $BaCl_2$, 140 mM

triethylammonium (TEA), 2 mM $MgCl_2$, 10 mM d-glucose, 10 mM Hepes (pH 7.3). The intracellular solution contained: 100 mM CsCl, 20 mM TEA, 10 mM EGTA, 10 mM Hepes, 5 mM MgATP, 1 mM $MgCl_2$, pH 7.3.

Voltage-clamp data were compiled and analyzed using IGOR Pro (WaveMetrics) and Excel (Microsoft). Peak $I_{Ca,L}(Ba^{2+})$ was measured during 300 ms depolarization from a holding potential of −50 mV to potentials between −50 and 50 mV. $I_{Ca,L}$ density (pA/pF) was defined as the peak current elicited by the voltage depolarization normalized to the whole-cell membrane capacitance within the same myocyte. Data are presented as mean ± SE. Statistical significance was evaluated using paired Student *t* test (Fig. 4 *A*–*C*) or one-way ANOVA with Bonferroni's post hoc test (Fig. 4*D*).

Ca^{2+} Transients. Intracellular Ca^{2+} was measured in isolated adult ventricular cardiomyocytes essentially as described (49). Cells were loaded for 30 min with the fluorescent Ca^{2+} indicator Fluo-4 AM (Molecular Probes) before being allowed to settle onto a glass coverslip. Cells were paced at 1 Hz and continuously perfused with external control solution with or without ISO. Fluorescence was detected using a Bio-Rad Radiance 2000 system attached to a Nikon TE300 inverted microscope with 60× oil immersion lens and operated by Lasersharp 2000 (v. 4.0) software. Images were further quantified using ImageJ. Ca^{2+} concentration was calculated from fluorescence intensity using the pseudoratio equation:

$$[Ca^{2+}]_i = K_d(F/F_0)\Big/\Big[K_d/[Ca^{2+}]_{i,\mathrm{rest}} + 1 - (F/F_0)\Big],$$

where K_d is the dissociation constant of Fluo-4 AM at 22 °C (770 nM), F is the fluorescence intensity, F_0 is the resting fluorescence, and $[Ca^{2+}]_{i,\mathrm{rest}}$ is the assumed resting Ca^{2+} concentration (100 nM).

ACKNOWLEDGMENTS. We thank Emma White for excellent technical assistance. This work was supported by National Institutes of Health (NIH) Grants R01 GM32875 (to G.S.M.), R01 HL088366 (to J.D.S.), and R01 HL085372 (to W.A.C.). NIH Grant T32 HL07312 (Experimental Pathology of Cardiovascular Disease) supported B.W.J., and the American Heart Association (National Scientist Development Award) supported S.B.

1. Diviani D, Dodge-Kafka KL, Li J, Kapiloff MS (2011) A-kinase anchoring proteins: Scaffolding proteins in the heart. *Am J Physiol Heart Circ Physiol* 301:H1742–H1753.
2. Carnegie GK, et al. (2008) AKAP-Lbc mobilizes a cardiac hypertrophy signaling pathway. *Mol Cell* 32:169–179.
3. Marx SO, et al. (2000) PKA phosphorylation dissociates FKBP12.6 from the calcium release channel (ryanodine receptor): Defective regulation in failing hearts. *Cell* 101: 365–376.
4. Chen L, et al. (2007) Mutation of an A-kinase-anchoring protein causes long-QT syndrome. *Proc Natl Acad Sci USA* 104:20990–20995.
5. Gray PC, Tibbs VC, Catterall WA, Murphy BJ (1997) Identification of a 15-kDa cAMP-dependent protein kinase-anchoring protein associated with skeletal muscle L-type calcium channels. *J Biol Chem* 272:6297–6302.
6. Fraser ID, et al. (1998) A novel lipid-anchored A-kinase Anchoring Protein facilitates cAMP-responsive membrane events. *EMBO J* 17:2261–2272.
7. Gray PC, et al. (1998) Primary structure and function of an A kinase anchoring protein associated with calcium channels. *Neuron* 20:1017–1026.
8. Henn V, et al. (2004) Identification of a novel A-kinase anchoring protein 18 isoform and evidence for its role in the vasopressin-induced aquaporin-2 shuttle in renal principal cells. *J Biol Chem* 279:26654–26665.
9. Trotter KW, et al. (1999) Alternative splicing regulates the subcellular localization of A-kinase anchoring protein 18 isoforms. *J Cell Biol* 147:1481–1492.
10. Hulme JT, Ahn M, Hauschka SD, Scheuer T, Catterall WA (2002) A novel leucine zipper targets AKAP15 and cyclic AMP-dependent protein kinase to the C terminus of the skeletal muscle Ca^{2+} channel and modulates its function. *J Biol Chem* 277:4079–4087.
11. Hulme JT, Lin TW, Westenbroek RE, Scheuer T, Catterall WA (2003) Beta-adrenergic regulation requires direct anchoring of PKA to cardiac CaV1.2 channels via a leucine zipper interaction with A kinase-anchoring protein 15. *Proc Natl Acad Sci USA* 100: 13093–13098.
12. Fuller MD, Emrick MA, Sadilek M, Scheuer T, Catterall WA (2010) Molecular mechanism of calcium channel regulation in the fight-or-flight response. *Sci Signal* 3:ra70.
13. Tibbs VC, Gray PC, Catterall WA, Murphy BJ (1998) AKAP15 anchors cAMP-dependent protein kinase to brain sodium channels. *J Biol Chem* 273:25783–25788.
14. Few WP, Scheuer T, Catterall WA (2007) Dopamine modulation of neuronal Na^+ channels requires binding of A kinase-anchoring protein 15 and PKA by a modified leucine zipper motif. *Proc Natl Acad Sci USA* 104:5187–5192.
15. Cantrell AR, Tibbs VC, Westenbroek RE, Scheuer T, Catterall WA (1999) Dopaminergic modulation of voltage-gated Na^+ current in rat hippocampal neurons requires anchoring of cAMP-dependent protein kinase. *J Neurosci* 19:RC21.
16. Lygren B, et al. (2007) AKAP complex regulates Ca^{2+} re-uptake into heart sarcoplasmic reticulum. *EMBO Rep* 8:1061–1067.
17. Singh A, Redden JM, Kapiloff MS, Dodge-Kafka KL (2011) The large isoforms of A-kinase anchoring protein 18 mediate the phosphorylation of inhibitor-1 by protein kinase A and the inhibition of protein phosphatase 1 activity. *Mol Pharmacol* 79:533–540.
18. Nicolaou P, Hajjar RJ, Kranias EG (2009) Role of protein phosphatase-1 inhibitor-1 in cardiac physiology and pathophysiology. *J Mol Cell Cardiol* 47:365–371.
19. Carr AN, et al. (2002) Type 1 phosphatase, a negative regulator of cardiac function. *Mol Cell Biol* 22:4124–4135.
20. Lemke T, et al. (2008) Unchanged beta-adrenergic stimulation of cardiac L-type calcium channels in $Ca_V1.2$ phosphorylation site S1928A mutant mice. *J Biol Chem* 283: 34738–34744.
21. Hulme JT, Westenbroek RE, Scheuer T, Catterall WA (2006) Phosphorylation of serine 1928 in the distal C-terminal domain of cardiac $Ca_V1.2$ channels during beta1-adrenergic regulation. *Proc Natl Acad Sci USA* 103:16574–16579.
22. Nichols CB, et al. (2010) Sympathetic stimulation of adult cardiomyocytes requires association of AKAP5 with a subpopulation of L-type calcium channels. *Circ Res* 107:747–756.
23. Hall DD, et al. (2007) Critical role of cAMP-dependent protein kinase anchoring to the L-type calcium channel $Ca_V1.2$ via A-kinase anchor protein 150 in neurons. *Biochemistry* 46:1635–1646.
24. Navedo MF, et al. (2008) AKAP150 is required for stuttering persistent Ca^{2+} sparklets and angiotensin II-induced hypertension. *Circ Res* 102:e1–e11.
25. Oliveria SF, Dell'Acqua ML, Sather WA (2007) AKAP79/150 anchoring of calcineurin controls neuronal L-type Ca^{2+} channel activity and nuclear signaling. *Neuron* 55:261–275.
26. MacLennan DH, Kranias EG (2003) Phospholamban: A crucial regulator of cardiac contractility. *Nat Rev Mol Cell Biol* 4:566–577.
27. Carr DW, Hausken ZE, Fraser ID, Stofko-Hahn RE, Scott JD (1992) Association of the type II cAMP-dependent protein kinase with a human thyroid RII-anchoring protein. Cloning and characterization of the RII-binding domain. *J Biol Chem* 267:13376–13382.
28. McConnell BK, et al. (2009) Disruption of protein kinase A interaction with A-kinase-anchoring proteins in the heart in vivo: Effects on cardiac contractility, protein kinase A phosphorylation, and troponin I proteolysis. *J Biol Chem* 284:1583–1592.
29. Patel HH, et al. (2010) Disruption of protein kinase A localization using a trans-activator of transcription (TAT)-conjugated A-kinase-anchoring peptide reduces cardiac function. *J Biol Chem* 285:27632–27640.
30. Christian F, et al. (2011) Small molecule AKAP-protein kinase A (PKA) interaction disruptors that activate PKA interfere with compartmentalized cAMP signaling in cardiac myocytes. *J Biol Chem* 286:9079–9096.
31. Gao T, et al. (1997) cAMP-dependent regulation of cardiac L-type Ca^{2+} channels requires membrane targeting of PKA and phosphorylation of channel subunits. *Neuron* 19:185–196.
32. Hundsrucker C, et al. (2006) High-affinity AKAP7delta-protein kinase A interaction yields novel protein kinase A-anchoring disruptor peptides. *Biochem J* 396:297–306.
33. Carnegie GK, Means CK, Scott JD (2009) A-kinase anchoring proteins: From protein complexes to physiology and disease. *IUBMB Life* 61:394–406.
34. Lygren B, Taskén K (2008) The potential use of AKAP18delta as a drug target in heart failure patients. *Expert Opin Biol Ther* 8:1099–1108.
35. Dodge-Kafka KL, Langeberg L, Scott JD (2006) Compartmentation of cyclic nucleotide signaling in the heart: The role of A-kinase anchoring proteins. *Circ Res* 98:993–1001.
36. Ruehr ML, Russell MA, Bond M (2004) A-kinase anchoring protein targeting of protein kinase A in the heart. *J Mol Cell Cardiol* 37:653–665.
37. Mauban JR, O'Donnell M, Warrier S, Manni S, Bond M (2009) AKAP-scaffolding proteins and regulation of cardiac physiology. *Physiology (Bethesda)* 24:78–87.
38. Marx SO, et al. (2001) Phosphorylation-dependent regulation of ryanodine receptors: A novel role for leucine/isoleucine zippers. *J Cell Biol* 153:699–708.
39. Marx SO, et al. (2002) Requirement of a macromolecular signaling complex for beta adrenergic receptor modulation of the KCNQ1-KCNE1 potassium channel. *Science* 295:496–499.
40. Baisamy L, Jurisch N, Diviani D (2005) Leucine zipper-mediated homo-oligomerization regulates the Rho-GEF activity of AKAP-Lbc. *J Biol Chem* 280:15405–15412.
41. Cantrell AR, et al. (2002) Molecular mechanism of convergent regulation of brain Na^+ channels by protein kinase C and protein kinase A anchored to AKAP-15. *Mol Cell Neurosci* 21:63–80.
42. Marshall MR, et al. (2011) Functional roles of a C-terminal signaling complex of Ca_V1 channels and A-kinase anchoring protein 15 in brain neurons. *J Biol Chem* 286: 12627–12639.
43. Willis BS, Niswender CM, Su T, Amieux PS, McKnight GS (2011) Cell-type specific expression of a dominant negative PKA mutation in mice. *PLoS ONE* 6:e18772.
44. Weisenhaus M, et al. (2010) Mutations in AKAP5 disrupt dendritic signaling complexes and lead to electrophysiological and behavioral phenotypes in mice. *PLoS ONE* 5:e10325.
45. Bregman DB, Bhattacharyya N, Rubin CS (1989) High affinity binding protein for the regulatory subunit of cAMP-dependent protein kinase II-B. Cloning, characterization, and expression of cDNAs for rat brain P150. *J Biol Chem* 264:4648–4656.
46. De Jongh KS, et al. (1996) Specific phosphorylation of a site in the full-length form of the alpha 1 subunit of the cardiac L-type calcium channel by adenosine 3′,5′-cyclic monophosphate-dependent protein kinase. *Biochemistry* 35:10392–10402.
47. O'Connell TD, Rodrigo MC, Simpson PC (2007) Isolation and culture of adult mouse cardiac myocytes. *Methods Mol Biol* 357:271–296.
48. Brunet S, Scheuer T, Catterall WA (2009) Cooperative regulation of $Ca_V1.2$ channels by intracellular Mg^{2+}, the proximal C-terminal EF-hand, and the distal C-terminal domain. *J Gen Physiol* 134:81–94.
49. Santana LF, Chase EG, Votaw VS, Nelson MT, Greven R (2002) Functional coupling of calcineurin and protein kinase A in mouse ventricular myocytes. *J Physiol* 544:57–69.